ORIGINAL RESEARCH

Single-Beat Estimation of Right Ventricular Contractility and Its Coupling to Pulmonary Arterial Load in Patients With Pulmonary Hypertension

Ryo Inuzuka, MD, PhD; Steven Hsu, MD; Ryan J. Tedford, MD; Hideaki Senzaki, MD, PhD

***Background*—**An accurate assessment of intrinsic right ventricular (RV) contractility and its relation to pulmonary arterial load is essential for the management of pulmonary hypertension. The pressure-volume relationship with load manipulation is the gold standard assessment used for this purpose, but its clinical application has been hindered by the lack of a single-beat method that is valid for the human RV. In the present study, we sought to validate a novel single-beat method to estimate the preload recruitable stroke work (PRSW) and its derivative for ventriculoarterial coupling in the human RV.

***Methods and Results*—**A novel single-beat slope of the PRSW relationship (M_{sw}) was derived by calculating the mean ejection pressure when the end-systolic volume was equal to volume-axis intercept of the PRSW relationship. In addition, by using a mathematical transformation of the equation representing the linearity of the PRSW relationship, a novel index for ventriculoarterial coupling, M_{sw}/mean ejection pressure, was developed. RV pressure-volume relationships were measured in 31 patients (including 23 patients with pulmonary hypertension) who were referred for right-sided heart catheterization. In this cohort, the single-beat M_{sw} was strongly correlated with the multiple-beat M_{sw} (r=0.91, P<0.0001). Moreover, a significant correlation was observed between the single- and multiple-beat M_{sw}/mean ejection pressure (r=0.53, P=0.002), with a stronger correlation in those with greater RV systolic pressure (r=0.70, P=0.003).

***Conclusions*—**The novel single-beat approach provided an accurate estimation of indexes for the PRSW relationship and ventriculoarterial coupling. It may be particularly useful in assessing RV adaptation to increased pressure overload. **(*J Am Heart Assoc*. 2018;7:e007929. DOI: 10.1161/JAHA.117.007929.)**

Key Words: contractility • heart failure • pressure-volume relationship • pulmonary circulation • pulmonary hypertension • pulmonary impedance

Pulmonary arterial (PA) hypertension (PAH) can lead to pathologic remodeling of the pulmonary vasculature and progressive increases in the PA load. Although the right ventricle (RV) attempts to adapt by compensatory hypertrophy and dilation, adaptation can become insufficient, leading to right-sided heart failure and ultimately death.[1] Accordingly, prognosis in PAH is strongly related to RV compensation rather than to the degree of the vascular injury itself.[1–3] Thus, accurate assessment of intrinsic RV contractility and its relation to the PA load is essential for refining risk stratification and optimizing treatment in these patients.[1,3] However, commonly used indexes of RV contractility, such as the RV ejection fraction (EF) and tricuspid annular plane systolic excursion, are limited by considerable load dependence.[4]

Pressure-volume (PV) relationships provide relatively load-insensitive measures of contractility, such as end-systolic elastance (E_{es}), preload-recruitable stroke work (PRSW), and E_{es}/arterial elastance (E_a), a key metric that describes

From the Department of Pediatrics, University of Tokyo, Tokyo, Japan (R.I.); Division of Cardiology, Department of Medicine, Johns Hopkins School of Medicine, Baltimore, MD (S.H.); Division of Cardiology, Department of Medicine, Medical University of South Carolina, Charleston, SC (R.J.T.); Department of Pediatric Cardiology, Saitama Medical Center, Saitama Medical University, Saitama, Japan (H.S.); and Department of Pediatrics and Pediatric Cardiology, Kitasato University, Sagamihara, Kanagawa, Japan (H.S.).

Accompanying Data S1 through S3 and Figures S1 through S5 are available at http://jaha.ahajournals.org/content/7/10/e007929/DC1/embed/inline-supplementary-material-1.pdf

Correspondence to: Hideaki Senzaki, MD, PhD, Department of Pediatrics and Pediatric Cardiology, Kitasato University, IPE Building, Room 413, 1-15-1 Kitasato, Sagamihara, Kanagawa 252-0375, Japan. E-mail: hsenzaki@med.kitasato-u.ac.jp

Received October 23, 2017; accepted April 3, 2018.

Clinical Perspective

What Is New?

- Pulmonary impedance describes both steady and pulsatile afterloads, but it has been unable to be summarized by a single number. Right ventricular (RV) mean ejection pressure/stroke volume represents a comprehensive marker for pulmonary impedance.
- Balance between RV contractility and pulmonary arterial (PA) afterload (ie, RV-PA coupling) can be assessed using a simple index: preload recruitable stroke work/mean ejection pressure.
- Preload recruitable stroke work and its coupling to PA load can be estimated from a single beat without changing loading conditions, which can help improve the diagnosis and treatment of diseased RV in humans.

What Are the Clinical Implications?

- Whether preload recruitable stroke work–based RV-PA coupling index predicts clinical outcomes better than traditional RV-PA coupling indexes warrants future investigations.
- Molecular mechanisms of RV adaptation to pressure overload need to be studied further using the new preload recruitable stroke work–based measure of RV adaptation.

RV-PA coupling.[5–7] However, measuring E_{es} or PRSW requires generating a family of PV relationships over a wide range of volumes using means such as inferior vena cava occlusion or the Valsalva maneuver, which can be time-consuming and difficult to measure. Single-beat estimates of RV E_{es} have been proposed; however, these methods have not been validated for use in the human RV,[8–10] and unfortunately this estimate did not correlate with clinical outcomes in 2 recent studies.[11,12] The PRSW (M_{sw}), defined as the slope of ventricular stroke work (SW) versus end-diastolic volume measured across a range of ventricular volumes, arguably provides the most load-insensitive measure of RV contractility.[13] Compared with E_{es}, the PRSW relationship is reported to be more strictly linear, more reproducible, and less dependent on chamber size or afterload.[14] However, its clinical application has also been limited because of the lack of a single-beat method that is valid for the human RV.

We recently reported a novel single-beat approach for estimating M_{sw} in the canine left ventricle (LV).[15] This method may also be applicable to the human RV because it does not necessarily depend on conditions that are specific to the LV. In addition, we predicted, for the first time, that the M_{sw} could be coupled with ventricular afterload using a simple new index, M_{sw}/the mean ejection pressure (P_m), to assess RV-PA coupling. Thus, the present study sought to validate our novel single-beat method for M_{sw} and our newly described measure of RV-PA coupling in a cohort of subjects with invasively measured RV PV relationships.

Methods

The individual data will not be made available to other researchers for purposes of reproducing the results. The analytic methods, however, are presented as Supplementary Materials to assist other researchers in replicating the procedure.

Study Subjects

We retrospectively analyzed data from consecutive patients who underwent PV studies during right-sided heart catheterization for the diagnosis or management of pulmonary hypertension (PH) at the Johns Hopkins Hospital (Baltimore, MD) from November 1, 2012 to June 30, 2015. The research protocol was approved by Institutional Review Board of the Johns Hopkins School of Medicine, and informed consent was obtained from all patients.

PV Loop Analysis

After standard right-sided heart catheterization, a PV catheter (model SPC-570-2; Millar Instruments, Houston, TX) was advanced through the right internal jugular vein and positioned at the RV apex to measure instantaneous RV volume. The RV conductance signal was calibrated to match the RV EF, which was independently determined by same-day cardiac magnetic resonance imaging (CMR) and thermodilution cardiac output. PV loops and relationships were constructed both at baseline and during phase 2 of the Valsalva maneuver (period of preload decline), as validated previously.[10,16] PV data were digitalized at 500 Hz using a custom-designed data acquisition system and stored for subsequent offline analysis. Extraction of the conventional hemodynamic parameters from the PV loops was performed using custom analysis programs (WinPVAN-3.5.10). Further analyses involving multiple-beat E_{es} and PRSW were conducted using R version 3.0.1.

Calculation of E_{es} and the PRSW Relationship Using Multiple Beats

The end-systolic points for a series of loops during the Valsalva maneuver were determined as those with maximal elastance and were fitted against the linear end-systolic PV relationship (ESPVR) using the linear least-squares method, with the use of an iterative method to calculate the multiple-beat E_{es}, as previously reported.[17] Effective E_a was determined by dividing the end-systolic pressure by the stroke volume (SV), and RV-PA coupling was assessed as E_{es}/E_a. The PRSW relationship was also determined by a linear regression analysis of SW versus

end-diastolic volume data obtained during the Valsalva maneuver, according to the following equation:

$$SW = M_{SW} \times (V_{ed} - V_{SW}) \quad (1)$$

where M_{sw} and V_{sw} are the slope and volume-axis intercept, respectively.[13] The PRSW coefficients determined from multiple-beat data are specifically denoted as $M_{sw(MB)}$ and $V_{sw(MB)}$.

Outline of the Single-Beat Estimation of the ESPVR and the PRSW Relationship

Our single-beat approach for estimating RV M_{sw}, hereby described, involves the following: (1) an estimation of the ESPVR from the single-beat late systolic PV relation and (2) a determination of M_{sw} on the basis of a novel link between the PRSW relationship and the ESPVR. These have been validated previously for the LV in an animal study.[15]

(1) Estimation of the curvilinear ESPVR from the single-beat late systolic PV relation

We used a single-beat method to estimate a curvilinear ESPVR on the basis of the concept of maximum systolic myocardial stiffness, as previously proposed by Mirsky et al.[15,18] We modified the original ESPVR formula of Mirsky et al[18] to implement a CMR-measured wall volume into the formula, as outlined in detail in Data S1[19]:

$$P_{es}(V_{es}) = A \times \ln\left(\frac{V_{es}}{V_0}\right) \times \ln\left(1 + \frac{V_{wall}}{V_{es}}\right) \quad (2)$$

where A is an amplification factor and V_0 is the volume-axis intercept of the ESPVR, which represents the chamber volume when the fiber stress is assumed to be zero. The RV wall volume was measured using CMR or can be calculated from end-diastolic volume by assuming a constant RV wall-volume ratio when measured wall volume is not available. Figure 1 shows that the single-beat ESPVR was estimated by fitting the points between the peak systolic pressure and the end-systolic point on the signal-averaged baseline loop against equation 2 using the nonlinear least-squares method. This provides a zero-stress volume (V_0) on the basis of the single-baseline beat, which was denoted as $V_{0(SB)}$.

(2) Determination of M_{sw} from the estimated ESPVR

The principle for estimating the RV M_{sw} using a single beat is based on a novel physiologic link detected between the ESPVR and the PRSW relationships.[15] We defined the P_m as SW/SV:

$$SW = P_m \times SV \quad (3)$$

Combining equations 1 and 3 yields

$$P_m \times SV = M_{sw} \times (V_{es} + SV - V_{sw}) \quad (4)$$

which can be rearranged to

$$(P_m - M_{sw}) = \frac{M_{sw}}{SV} \times (V_{es} - V_{sw}) \quad (5)$$

More important, this equation indicates that when the end-systolic volume is equal to V_{sw}, P_m should be equal to M_{sw}. If one conceptualizes M_{sw} and V_{sw} as a PV coordinate, then the linearity of the PRSW relationship dictates that this coordinate (V_{sw}, M_{sw}), when placed on the PV plane, must be on the PV relationship between P_m and V_{es}, as defined in equation 5, which is hereby referred to as the end-systolic P_m-volume relationship (EMPVR) (see Figure 2A). This relationship is conceptually similar to the ESPVR, but with end-systolic pressure replaced by P_m. We assumed that the EMPVR: $P_m(V_{es})$ function has a curvilinear characteristic similar to that of the ESPVR:end-systolic pressure(V_{es}) (equation 2) with a common V_0 but a different amplification factor, as follows:

$$\begin{aligned} P_m(V_{es}) &= \frac{P_{m\_sb}}{P_{es}(V_{es\_sb})} \times P_{es}(V_{es}) \\ &= B \times \ln\left(\frac{V_{es}}{V_0}\right) \times \ln\left(1 + \frac{V_{wall}}{V_{es}}\right) \end{aligned} \quad (6)$$

where P_{m_sb} and V_{es_sb} are known P_m values and end-systolic volumes of the baseline single beat, respectively, and B is an amplification factor.

Once the ESPVR is estimated from a single beat, the EMPVR can also be determined as in equation 6 using $V_{0(SB)}$. As P_m is equal to M_{sw} when end-systolic volume is equal to V_{sw} [ie, $P_m(V_{sw})=M_{sw}$], substituting V_{sw} for V_{es} in equation 6 yields,

$$M_{sw} = B \times \ln\left(\frac{V_{sw}}{V_{0(SB)}}\right) \times \ln\left(1 + \frac{V_{wall}}{V_{sw}}\right) \quad (7)$$

Also, from equation 1,

$$SW_{sb} = M_{sw} \times (V_{ed\_sb} - V_{sw}) \quad (8)$$

where SW_{sb} and V_{ed_sb} are the known SW and end-diastolic volume of the baseline single beat, respectively. By solving the 2 simultaneous equations for M_{sw} and V_{sw} (equations 7 and 8), we finally obtain single-beat estimates of the PRSW coefficients ($M_{sw[SB]}$ and $V_{sw[SB]}$). A schematic flow chart using an example case for single-beat estimation of M_{sw} is summarized in Figure 2B. An algorithm using this outlined approach was generated in R version 3.0.1 (R Foundation) and used to calculate the M_{sw} uniformly from each signal-averaged single-beat loop.

Proposal of a Novel Index of Ventriculoarterial Coupling

We propose the use of the ratio of contractility (ie, the M_{sw}) to P_m as a novel index of RV-PA coupling. By rearranging equation 5, we obtain

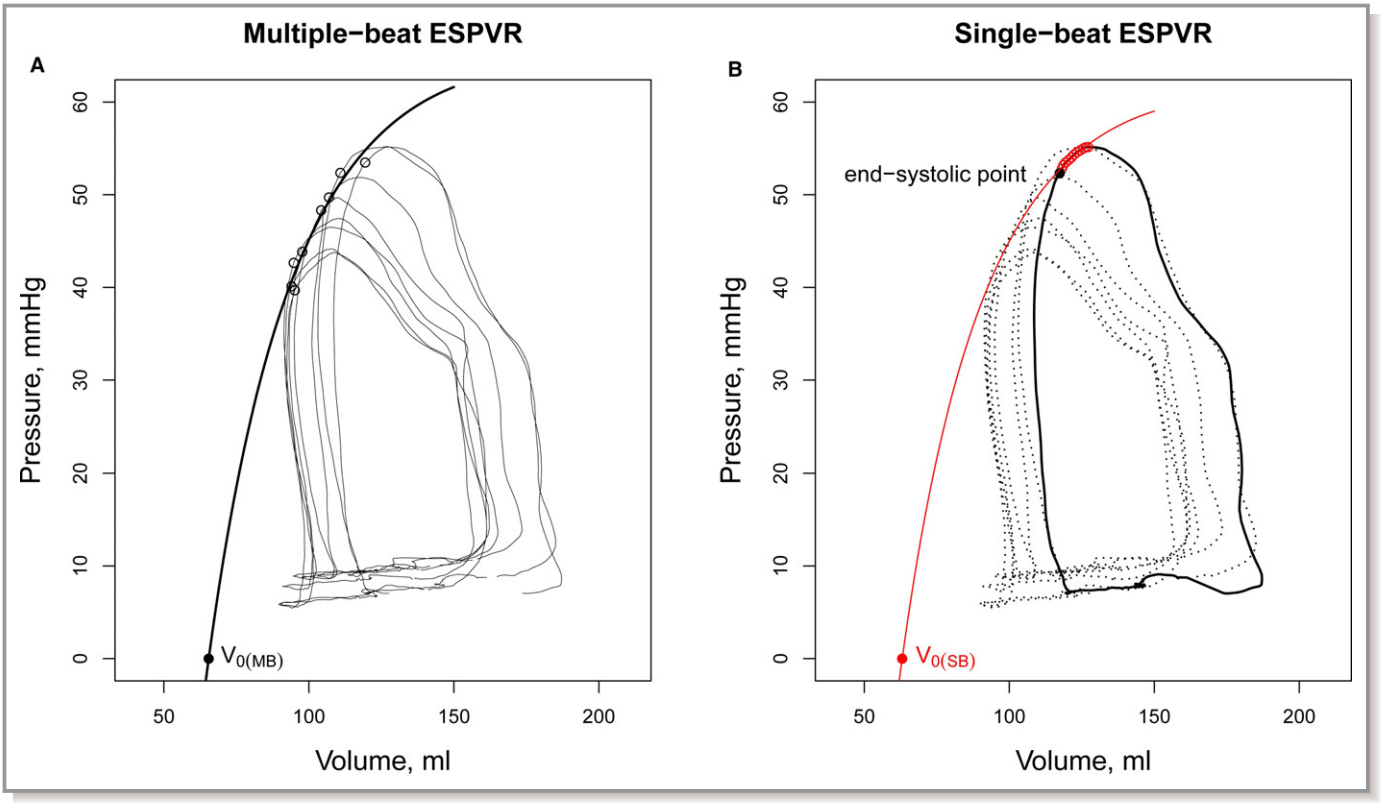

Figure 1. Single-beat estimation of the end-systolic pressure-volume relationship (ESPVR). A, Multiple-beat ESPVR (black curve). The end-systolic points for a series of loops were determined as those with maximal stress/strain ratio (open black circles) and were fitted against the equation for the ESPVR ($P = A \times \ln(\frac{V}{V_0}) \times \ln(1 + \frac{V_{wall}}{V})$) using a nonlinear least-square method, with the use of an iterative method to determine the zero-stress volume, $V_{0(MB)}$. B, Single-beat ESPVR (red curve) was estimated by fitting points between the peak systolic pressure and the end-systolic points (red open points) on the signal-averaged baseline loop against the equation, $P = A \times \ln(\frac{V}{V_0}) \times \ln(1 + \frac{V_{wall}}{V})$ (equation 2 in the main text) using the nonlinear least-squares method. The end-systolic point (ie, the last point used for the curve fitting; black closed point) in this figure has been determined uniformly using an algorithm on the basis of an iterative method, as described in detail in Figure S5. The red closed point represents the zero-stress volume of the single-beat ESPVR ($V_{0[SB]}$).

$$\frac{M_{sw}}{SV} = \frac{(P_m - M_{sw})}{(V_{es} - V_{sw})} = E'_{es} \quad (9)$$

where $\frac{(P_m - M_{sw})}{(V_{es} - V_{sw})}$ represents the local slope of the EMPVR and is denoted as E'_{es}, as shown in Figure 3. More important, equation 9 indicates that E'_{es} is consistently equal to the M_{sw} adjusted by the SV (ie, contractility). On the other hand, pulmonary vascular impedance can be represented by the slope of a diagonal line across the rectangular PV loop, as in Figure 3, which is denoted as E'_a:

$$E'_a = \frac{P_m}{SV} = \frac{SW}{SV^2} \quad (10)$$

As shown in Data S2, E'_a is transformed into an integrated form of vascular impedance on the basis of the concept that the external ventricular work (ie, SW) is equal to the hydraulic energy imparted to the blood.[1,20] The pumping performance of the ventricle can be determined by E'_{es}/E'_a in a similar way to E_{es}/E_a coupling, as shown in Figure 3.[7] Thus, this novel $E'_{es} - E'_a$ coupling framework, on the basis of the EMPVR, directly relates the intrinsic contractility with the vascular impedance. Multiplying both sides of equation 9 by SV/P_m yields

$$\frac{M_{sw}}{P_m} = \frac{(P_m - M_{sw})}{(V_{es} - V_{sw})} / \frac{P_m}{SV} = \frac{E'_{es}}{E'_a} \quad (11)$$

Therefore, the M_{sw} can be linked with the arterial load simply as M_{sw}/P_m to determine the RV-PA coupling (E'_{es}/E'_a) in the PV plane. Single- and multiple-beat M_{sw}/P_m were calculated as $M_{sw[SB]}/P_m$ and $M_{sw[MB]}/P_m$, respectively.

Statistical Analysis

Data were presented as mean±SD. The PRSW estimates, on the basis of the single-beat approach, were compared with the multiple-beat PRSW measurements (ie, the $V_{sw[MB]}$ and $M_{sw[MB]}$) using Pearson's correlation coefficient and a linear regression analysis. Bland-Altman analysis was used to assess

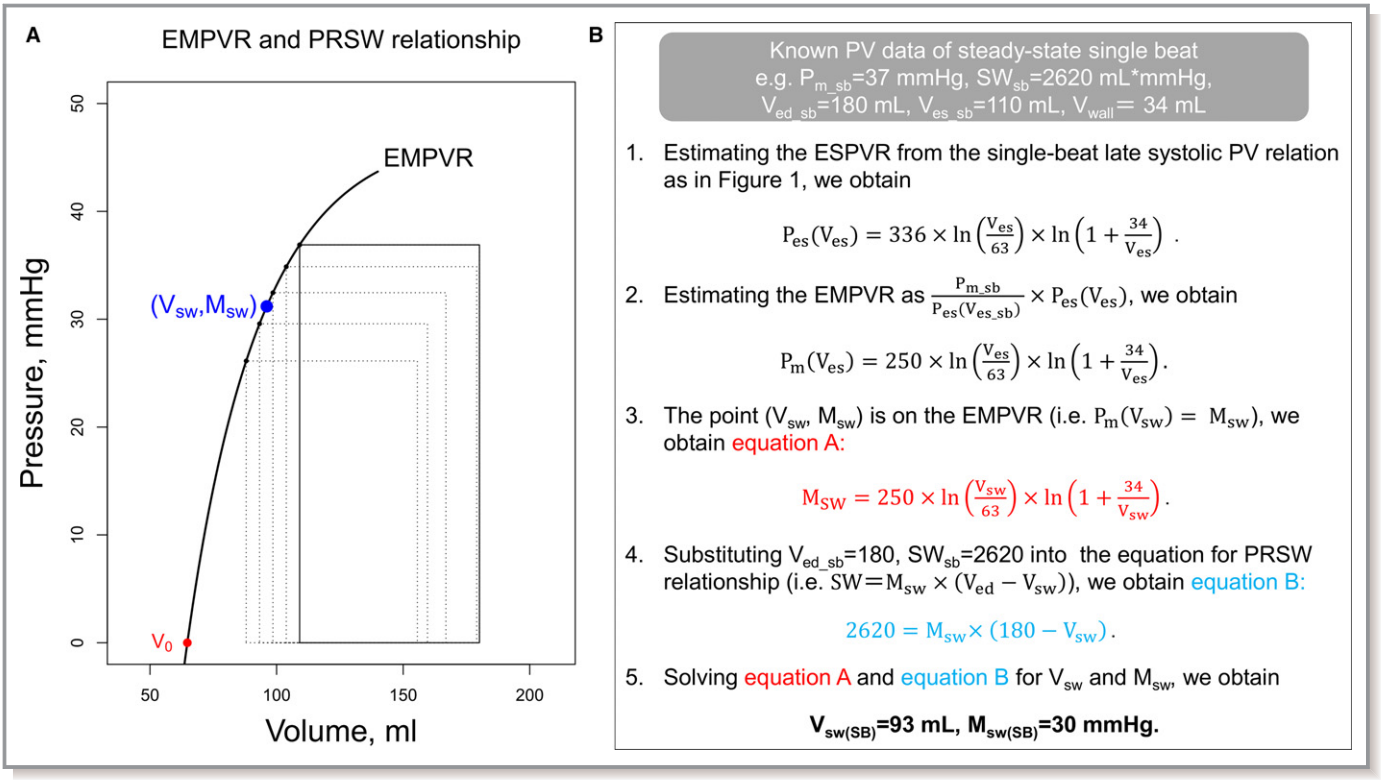

Figure 2. Outline of the single-beat estimation of the preload recruitable stroke work relationship. A, A novel physiologic feature that links the end-systolic mean ejection pressure (P_m)-volume relationship (EMPVR) and the preload recruitable stroke work (PRSW) relationship. The squares represent the rectangular-transformed pressure-volume (PV) loops that have the same area (ie, stroke work [SW]) and width (ie, stroke volume [SV]) as the original PV loops. The trajectory of the left-upper corners of the squares was denoted as the EMPVR. The bottoms of the squares were aligned at the volume axis; hence, the height of the square represents the absolute value of the P_m (SW/SV). The units for volume-axis and the slope of the PRSW relationship (V_{sw} and M_{sw}) are mL and mm Hg, respectively. When the point (V_{sw}, M_{sw}) is plotted as a blue point on the PV plane, this point is on the EMPVR curve, as demonstrated mathematically in the main text. B, Schematic flow chart of an example of single-beat estimation of M_{sw}. The P_m of the baseline single beat (P_{m_sb}=37 mm Hg) was calculated as the SW of the baseline single beat (SW_{sb}=2620 mL×mm Hg) divided by the SV of the baseline single beat (=70 mL). The right ventricular wall volume (V_{wall}) was obtained from the cardiac magnetic resonance imaging. ESPVR indicates end-systolic pressure-volume relationship; $M_{sw(SB)}$, slope of the PRSW relationship estimated from the baseline single beat; V_0, volume-axis intercept of the ESPVR; V_{ed_sb}, end-diastolic volume of the baseline single beat; V_{es_sb}, end-systolic volume of the baseline single beat; and $V_{sw(SB)}$, volume-axis intercept of the PRSW relationship estimated from the baseline single beat.

the agreement between single- and multiple-beat measurements. Statistical analyses were conducted with R version 3.0.1.[21]

Results

Study Population

Of the 41 patients enrolled, we evaluated data from 31 who had successful studies for PV loops and CMR (6 patients did not complete the study for safety or technical reasons, and 4 patients were excluded because of insufficient preload reduction with the Valsalva maneuver). The analyzed cohort included 23 patients with PH (idiopathic PAH, n=6; systemic sclerosis PAH, n=13; systemic sclerosis with PH attributable to heart failure with preserved EF or interstitial lung disease, n=4) and 8 patients without PH (systemic sclerosis without PH, n=6; no PH, n=2). Patient characteristics are shown in Table 1.

Multiple-beat data

Table 2 shows that the PV data were obtained from patients with variable hemodynamic statuses. The RV end-diastolic wall-to-chamber volume ratio was 0.17±0.06. During phase 2 of the Valsalva maneuver, 6.0±2.2 PV loops were obtained. Variable multiple-beat E_{es} (0.14–1.9 mm Hg/mL) and E_a (0.29–2.3) resulted in variable RV-PA coupling ($E_{es}/E_{a[MB]}$), which ranged from 0.23 to 4.5 (1.0±0.91). The PRSW relationship was highly linear (r=0.97±0.02), and the $M_{sw(MB)}$ ranged from 14 to 64 mm Hg. The ratio between $M_{sw(MB)}$ and P_m ($M_{sw[MB]}/P_m=E'_{es}/E'_a$), our novel index of RV-PA coupling,

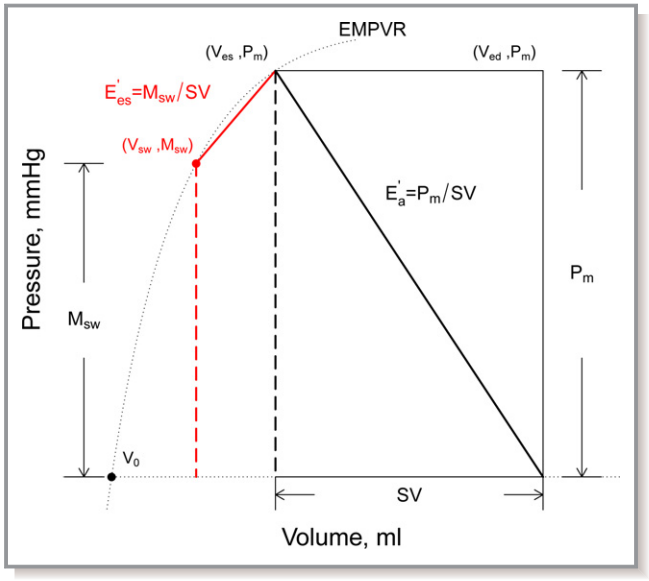

Figure 3. A novel ventriculoarterial coupling framework on the basis of the end-systolic mean ejection pressure (P_m)-volume relationship (EMPVR). If the preload recruitable stroke work relationship can be assumed to be linear, E'_{es}, the slope of the red segment between the end-systolic point of the baseline square (V_{es}, P_m) and the point (volume-axis intercept of the preload recruitable stroke work [PRSW] relationship [V_{sw}], slope of the PRSW relationship [M_{sw}]) is equal to $\frac{M_{sw}}{SV}$, as shown in equation 9 in the text. Moreover, the effective arterial elastance for the rectangular pressure-volume loop ($E'_a = \frac{P_m}{SV}$, black slope) represents the vascular impedance that accounts for both steady and pulsatile afterload, as shown in Data S2. The pump performance of the ventricle can be determined by E'_{es}/E'_a in a similar way to E_{es}/E_a. Furthermore, E'_{es}/E'_a can be simply formulated as M_{sw}/P_m, as shown in equation 11 in the text. SV indicates stroke volume.

was 0.75±0.16. The $M_{sw(MB)}/P_m$ (=E'_{es}/E'_a) ranged from 0.51 to 1.17, as a result of variable E'_{es} ($M_{sw[MB]}$/SV, range, 0.18–1.3) and E'_a (=P_m/SV, range, 0.23–1.7). Although both indexes of RV-PA coupling ($E_{es}/E_{a[MB]}$ and $M_{sw[MB]}/P_m$) were significantly correlated with each other (r=0.53, P=0.002, Figure S1), the range of change differed considerably. The RV-PA coupling ratio in patients with PH was significantly lower than that in those without PH (P=0.03 for multiple-beat E_{es}/E_a, and P=0.003 for $M_{sw[MB]}/P_m$).

Single-beat estimation of the PRSW relationship and RV-PA coupling

An iterative algorithm yielded an average of 20 points (range, 9–56 points) on a steady-state PV loop to be used for single-beat ESPVR estimation. Figure 4 shows that the zero-stress volumes of the single- and multiple-beat ESPVRs were strongly correlated (r=0.86, P<0.0001). The single-beat estimation of the PRSW slope ($M_{sw[SB]}$) estimated from the signal-averaged baseline PV loop was strongly correlated with

Table 1. Patient Characteristics

Characteristics	Value (n=31)
Diagnoses, n (%)	
IPAH	6 (19.4)
SSc-PAH	13 (42.0)
SSc-PH attributable to HFpEF or ILD	4 (12.9)
SSc without PH	6 (19.4)
No PH	2 (6.5)
Age, y	61±12
Female sex, n (%)	28 (90)
Body surface area, m^2	1.84±0.21
NYHA class III/IV, n (%)	12 (39)
Heart rate, bpm	74±13
Systemic arterial pressure, mm Hg	94±14

Continuous variables are shown as mean±SD. Bpm indicates beats per minute; HFpEF, heart failure with preserved ejection fraction; ILD, interstitial lung disease; IPAH, idiopathic PAH; NYHA, New York Heart Association; PAH, pulmonary arterial hypertension; PH, pulmonary hypertension; SSc, systemic sclerosis.

the multiple-beat PRSW slope, $M_{sw(MB)}$ (Figure 5A, r=0.91, P<0.0001). Even when the RV end-diastolic wall-to-chamber volume ratio was assumed (a mean value of 0.17), the single-beat approach provided an accurate estimation of $M_{sw(MB)}$ without individual information on the RV wall volume (Figure 5B, r=0.91, P<0.0001). Bland-Altman plots showed a mild overestimation by 3.7 (SEM, 0.92) mm Hg and limits of agreement from −6.5 to 14.0 mm Hg (Figure 5C and 5D).

Although estimated and measured E'_{es} (ie, $M_{sw[SB]}$/SV and $M_{sw[MB]}$/SV) strongly correlated with each other (r=0.95, P<0.0001, Figure S2), the correlation between estimated and measured RV-PA coupling on the basis of the E'_{es} (ie, single- versus multiple-beat E'_{es}/E'_a calculated as $M_{sw[SB]}/P_m$ versus $M_{sw[MB]}/P_m$) was only moderate (r=0.52, P=0.002, Figure 6A), with a stronger correlation in patients with greater RV systolic pressure (red circles; RV pressure ≥ median of 44.12 mm Hg, r=0.68, P=0.004). Even when the $M_{sw(SB)}$ on the basis of the assumed RV end-diastolic wall-to-chamber volume ratio was used to estimate RV-PA coupling, the correlation between estimated and measured RV-PA coupling was moderate (r=0.53, P=0.002), with a stronger correlation in those with greater RV systolic pressure (r=0.70, P=0.003), as shown in Figure 6B.

Validation analyses for our single-beat method

To test the validity of the basic principle of our estimation method that the point (V_{sw}, M_{sw}) is on the EMPVR curve, PRSW coefficients that were determined from the multiple-beat EMPVR (as a point on the EMPVR) were compared with the actual multiple-beat PRSW coefficients (ie, $M_{sw[MB]}$ and

$V_{sw[MB]}$). The actual and EMPVR-based PRSW coefficients derived from the same set of multiple-beat data were robustly correlated with each other (r=0.98, P<0.0001 for V_{sw} and r=0.99, P<0.0001 for M_{sw} estimation, Figure S3). More important, a similar analysis, assuming that the EMPVR was linear, reduced the robustness (r=0.93 for M_{sw} and r=0.56 for V_{sw}), which highlights both the importance of selecting an appropriate EMPVR model and the validity of our model (equation 6).

Finally, as a sensitivity analysis, our single-beat method was applied to the first PV loop during phase 2 of the Valsalva maneuver, instead of the signal-averaged baseline PV loop. A strong correlation was still observed between the estimated and measured M_{sw} (r=0.89, P<0.0001).

Discussion

The present study showed, for the first time, that the slope of the PRSW relationship (ie, M_{sw}) can be accurately estimated from a single beat in the human RV by combining the following: (1) an estimation of the curvilinear ESPVR and EMPVR from the late-systolic PV relationship and (2) a novel physiologic link between the EMPVR and PRSW relationship (which identifies the M_{sw} by determining the P_m when the end-systolic volume is equal to V_{sw}). Moreover, our single-beat approach is the first to successfully link the M_{sw} with the impedance of the vascular system to generate the ratio M_{sw}/P_m, thereby providing a simple yet reliable estimate of RV-PA coupling. These attractive features of our single-beat method should be of great clinical value for the assessment of RV contractile function and RV-PA coupling, and thus can help improve the diagnosis and treatment of diseased RV in humans.

Table 2. Hemodynamic Data

Variable	Total (n=31)
Conventional right-sided heart catheterization data	
Cardiac output by thermodilution, L/min	4.70±0.91 (2.8–6.3)
Pulmonary arterial pressure, mm Hg	31±13 (14–67)
Pulmonary arterial wedge pressure, mm Hg	10±4.0 (4.0–19)
Pulmonary vascular resistance, Wood units	4.8±3.8 (1.2–19)
RV systolic pressure, mm Hg	50±22 (26–109)
RV end-diastolic pressure, mm Hg	11±5.2 (2.1–21)
dP/dt_{max}, mm Hg/s	441±131 (305–937)
Cardiac magnetic resonance imaging data	
RV end-diastolic volume, mL	144±40 (71–245)
RV ejection fraction, %	53±9.1 (34–71)
RV wall volume, mL	22.8±6.64 (12.8–40.6)
RV pressure-volume study data	
Multiple-beat E_{es}, mm Hg/mL	0.64±0.43 (0.14–1.9)
E_a, mm Hg/mL	0.80±0.45 (0.29–2.3)
Multiple-beat E_{es}/E_a	1.0±0.91 (0.23–4.5)
Stroke work, mm Hg/mL	2465±1064 (881–5200)
Multiple-beat M_{sw}, mm Hg	27±12 (14–64)
Multiple-beat V_{sw}, mL	50±23 (8.1–97)

Continuous variables are shown as mean±SD (range). dP/dt_{max} indicates maximum rate of RV pressure increase; E_a, effective arterial elastance; E_{es}, end-systolic elastance; M_{sw}, the slope of the preload recruitable stroke work relationship; RV, right ventricular; V_{sw}, x-axis intercept of the preload recruitable stroke work.

Single-Beat Estimation of Human RV E_{es} and M_{sw}

Assessment of RV function is increasingly recognized because of growing recognition that RV function is strongly related to outcomes in several cardiovascular diseases, including PH, congenital heart disease, and left-sided heart failure.[2] However, commonly used clinical indexes of RV contractility, such as RV EF or tricuspid annular plane systolic excursion, are limited by their considerable load dependence.[4] Both E_{es} and M_{sw} provide measures of an intrinsic contractile state that are largely independent of loading conditions, even for the RV,[6,14] but the clinical application of these indexes has been extremely limited by the need to record multiple beats over a wide volume range. Although several single-beat methods for such indexes have been developed and validated for the LV,[17,22] the application of such methods to the RV has not

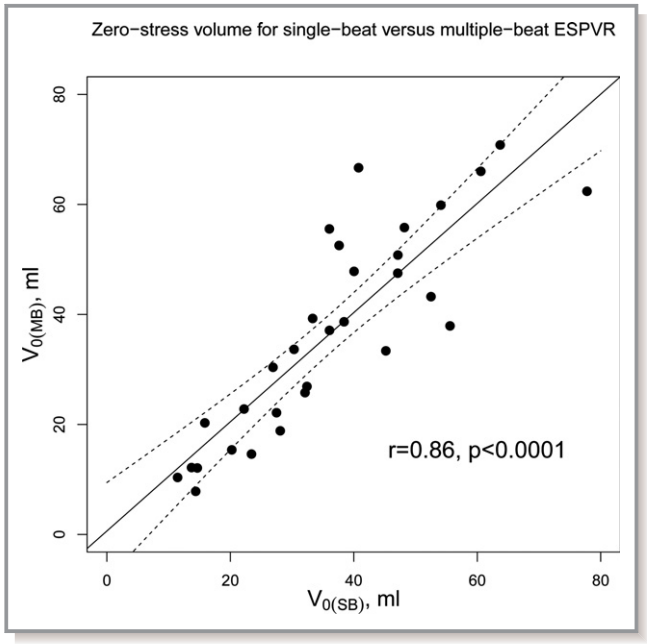

Figure 4. Single- and multiple-beat end-systolic pressure-volume relationship (ESPVR). Scatterplots comparing zero-stress volumes of single- vs multiple-beat ESPVRs ($V_{0[SB]}$ and $V_{0[MB]}$, respectively).

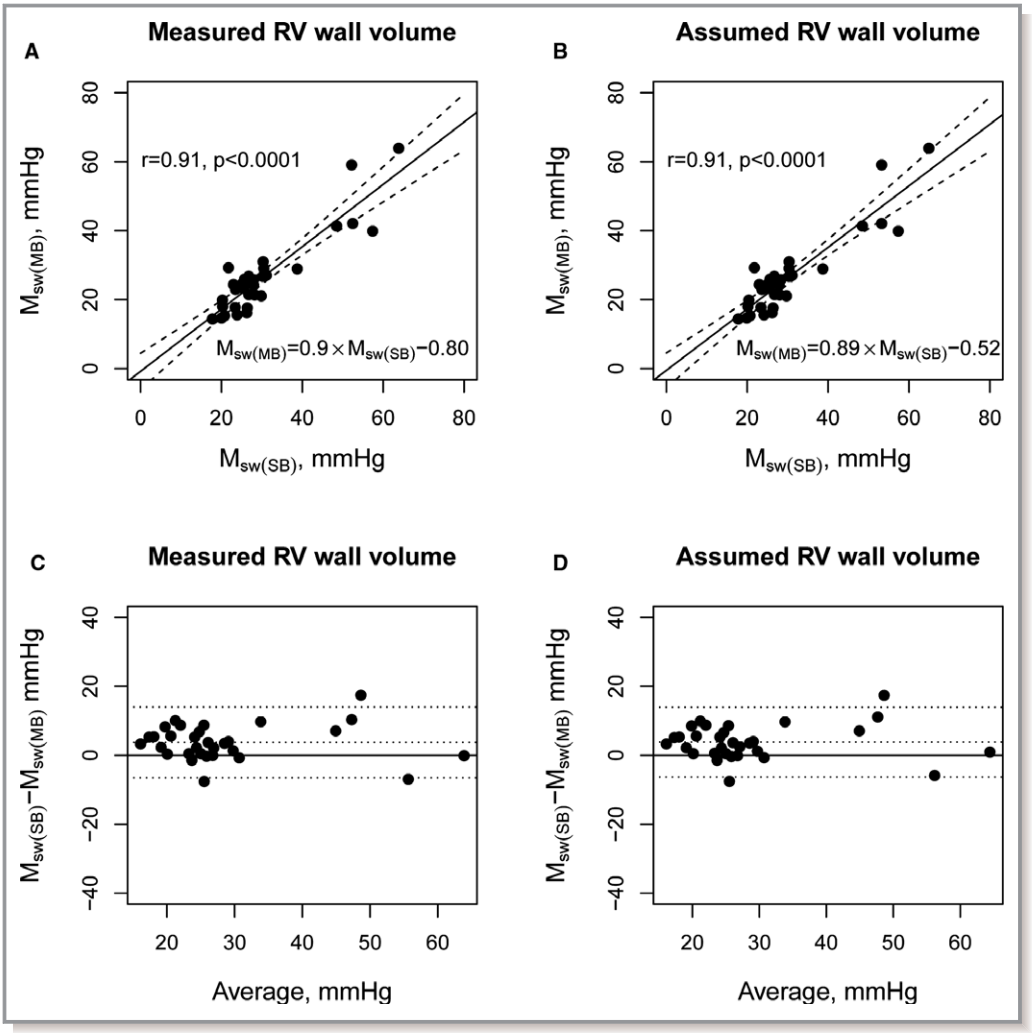

Figure 5. Estimated and measured preload recruitable stroke work slope, M_{sw}. A, Scatterplots comparing the estimated preload recruitable stroke work (PRSW) slope ($M_{sw[SB]}$) on the basis of the single-beat method using measured right ventricular wall volume to the multiple-beat PRSW slope ($M_{sw[MB]}$). B, Similar analysis using the assumed right ventricular (RV) end-diastolic wall/chamber volume ratio. C, Bland-Altman plots for $M_{sw(SB)}$ on the basis of the single-beat method using measured RV wall volume. D, Bland-Altman plots for $M_{sw(SB)}$ using the assumed RV end-diastolic wall/chamber volume ratio.

necessarily been successful in the human RV. A single-beat approach for estimating E_{es} using the sine-wave fit, originally developed for the LV by Sunagawa et al,[23,24] is believed to work for the RV. This belief is based on indirect evidence from an animal study that the maximal pressure of isovolumetric contraction (during pulmonary artery clamping) can be predicted from sine-wave fitting of the isovolumetric phase of RV pressure.[8] However, this single-beat method has never been validated in the human RV and was shown to agree poorly with measured E_{es} in an animal study.[25] Furthermore, this estimate was not found to be associated with clinical outcomes in 2 recent studies.[11,12]

This is the first study to demonstrate a single-beat method that is valid for use in the human RV. We used a novel approach to estimate both the ESPVR and PRSW relationship, which has already been validated for the LV in our animal study.[15] Because the ESPVR and PRSW relationships have different hemodynamic characteristics, using both relationships would be ideal to enhance clinical interpretation. The curvilinear ESPVR used in the present study is based on the concept proposed by Mirsky et al that the maximal myocardial stiffness (ie, stress/strain ratio of the ventricular wall) attained at end systole is constant throughout short-term changes in preload and afterload.[18] The estimation of ESPVR from the late systolic PV relation is based on the notion that the late systolic PV relation can be approximated as a set of PV data achieving maximal myocardial stiffness (ie, ESPVR).[15] In fact, in our RV data, a near-maximal myocardial stiffness (97.7% of the maximal myocardial stiffness on average) was already attained during late systole (ie, before end systole),

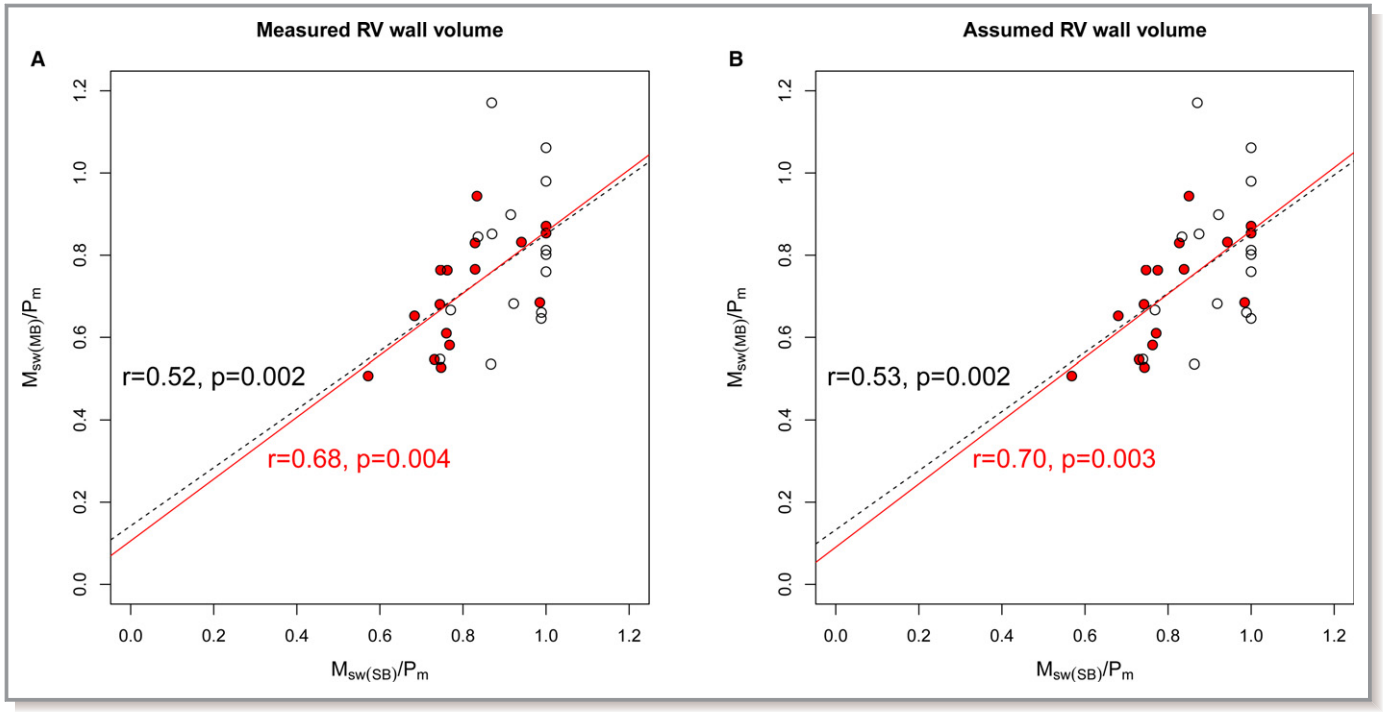

Figure 6. Single-beat estimation of a novel index of right ventricular–pulmonary arterial coupling. A, Scatterplots comparing single- and multiple-beat slope of the preload recruitable stroke work (PRSW) relationship (M_{sw})/mean ejection pressure (P_m), calculated using measured right ventricular (RV) wall volume. A stronger correlation was observed in those with greater RV systolic pressure (median of 44 mm Hg or greater; closed red points). B, Similar analysis using the assumed RV end-diastolic wall/chamber volume ratio. $M_{sw(MB)}$ indicates the multiple-beat PRSW slope; and $M_{sw(SB)}$, the estimated PRSW slope from a single beat.

which supports the use of a late systolic PV relation to estimate ESPVR in the human RV. Although the late systolic period can be short in some patients with PH, sufficient data acquisition for curve fitting was possible in the present study. We showed that the V_0 of the ESPVR can be accurately estimated using 20 data points on average (range, 9–56 points). Although curvilinear ESPVR models have been shown to provide a more reliable trajectory of the ESPVR than linear ESPVR,[18,26] it has not been widely acknowledged because it does not provide single numbers for contractility and for ventriculoarterial coupling, such as E_{es} and E_{es}/E_a. However, in the present study, because of a novel link between the ESPVR and the PRSW relationship that has been validated for the first time in the RV, the curvilinear ESPVR model was able to provide another load-insensitive measure of contractility, the M_{sw}. Because the M_{sw} has many advantages over E_{es}, including its strong linearity over a wide range of physiologic loads and independence of chamber size and volume signal gain, our single-beat method may be of great clinical value in assessing RV contractility in diseases of the right side of the heart.

Assessment of RV-PA Coupling Using the M_{sw}

Despite the attractive features of the M_{sw}, as previously noted, one important limitation of the M_{sw} thus far has been the inability to relate it to PA loads in the PV plane to assess RV-PA coupling. In the present study, we have resolved this long-standing problem with the M_{sw} by developing a novel index of M_{sw}-based RV-PA coupling: M_{sw}/P_m, which is equal to the E'_{es}/E'_a in the PV plane. Figure 3 shows that E'_{es} is the local slope of the EMPVR, which is analogous to a linear approximation of the curvilinear ESPVR and reflects intrinsic contractility (ie, M_{sw} adjusted by SV). More important, the afterload (E'_a) that is coupled with the E'_{es} represents an integrated form of vascular impedance (Data S2), which is known to provide a comprehensive description of both steady and pulsatile afterloads (including PA resistance and compliance). Thus, the $E'_{es} - E'_a$ framework is physically meaningful because it is derived mathematically from well-established measures of contractility and vascular load. This is in contrast to the E_{es}-E_a framework, wherein E_a is only indirectly related to vascular impedance.[27] By considering P_m, rather than end-systolic pressure (ie, at EMPVR rather than at ESPVR), one can assess RV-PA coupling on the basis of E'_{es}/E'_a, in a similar way to E_{es}/E_a. Although a minor difference between end-systolic pressure and P_m is expected in the LV, where the pulsatile component of the external ventricular power is far less than the steady component, a significant difference would exist for the RV, where the pulsatile power is reported to account for as much as 23% of the total ventricular power.[20] This was clearly shown by only a moderate correlation (r=0.53) and a

considerable difference in the range of change between multiple-beat E_{es}/E_a and E'_{es}/E'_a (ie, $E_{es}/E_{a[MB]}$ and $M_{sw}/P_{m[MB]}$), as shown in Figure S1. We speculate that the optimal value for the novel index of RV-PA coupling is ≈0.8 to 1.0, which was attained by those without PH (Figure S1). Although E_{es}/E_a is an established marker of RV-PA coupling, E'_{es}/E'_a potentially provides an even better characterization of RV-PA coupling, considering the significantly pulsatile PA load caused by enhanced PA wall stiffness and its substantial impact on survival in PAH.[28] Because survival in PAH is closely related to RV adaptation to the increased pressure overload (ie, RV-PA coupling),[1] whether the PRSW-based RV-PA coupling index (ie, M_{sw}/P_m or E'_{es}/E'_a) predicts clinical outcomes better than the traditional RV-PA coupling indexes, such as RV EF or an ESPVR-based index (E_{es}/E_a), warrants future investigations.

In the present study, although the agreement between estimated and measured E'_{es} on the basis of our single-beat method was excellent, the correlation between measured and estimated RV-PA coupling on the basis of the E'_{es} was only moderate for the whole population. This was mainly because the estimation of RV-PA coupling was less accurate in those with low afterload, wherein a small estimation error in contractility would result in a relatively large estimation error in RV-PA coupling (ie, ratio of contractility/afterload). However, RV-PA coupling is of clinical issue for those with elevated RV pressure in the setting of PH. For such patients, our single-beat method provided a better estimation of RV-PA coupling (r=0.70).

Study Limitations

First, this was a retrospective single-center study that enrolled a comparatively small number of patients. The sensitivity of our single-beat M_{sw} to short-term changes in inotropic status was not investigated in the present study, which needs to be elucidated in future investigations. Second, the formula used for modeling the curvilinear ESPVR in the present study was developed under the assumption of the ventricular shape to be prolate spheroid, and thus, the applicability of such a formula to the RV was not guaranteed.[19] However, our single-beat approach was capable of estimating the M_{sw} much more accurately than those based on a generally used linear ESPVR model, which provides strong evidence for the validity of our model. In addition, our single-beat method has an advantage of allowing selection of any other ESPVR formulas for further refinement. Third, the algorithm of our single-beat method may be somewhat complicated compared with that of the conventional single-beat method for E_{es} using sine-wave fitting. However, when the conventional sine-wave fit was applied to our data,[8,25] the correlation between single- and multiple-beat E_{es} was low (r=0.41), as shown in Figure S4, which would preclude a reliable assessment of contractility. A program to automate the data processing of our single-beat method is provided in Data S3 for the readers' wide use. Finally, our single-beat approach still requires measurement of instantaneous PV data. A combination of the pressure recording of the normal right-sided heart catheterization and flow/volume data on CMR would possibly provide a good approximation of the late systolic PV relation as well as the baseline SW necessary for our single-beat approach. This needs further study.

Conclusions

A load-insensitive measure of contractility, M_{sw}, for the human RV and its coupling to PA afterloads can be accurately estimated using our single-beat approach. This approach would help in precisely assessing RV adaptation to increased pressure overload and thereby help improve the management of patients with PH.

Acknowledgments

We thank Professor David Kass at Johns Hopkins School of Medicine for providing the PV data and valuable advice for the present study.

Disclosures

None.

References

1. Vonk-Noordegraaf A, Haddad F, Chin KM, Forfia PR, Kawut SM, Lumens J, Naeije R, Newman J, Oudiz RJ, Provencher S, Torbicki A, Voelkel NF, Hassoun PM. Right heart adaptation to pulmonary arterial hypertension: physiology and pathobiology. *J Am Coll Cardiol*. 2013;62:D22–D33.
2. Voelkel NF, Quaife RA, Leinwand LA, Barst RJ, McGoon MD, Meldrum DR, Dupuis J, Long CS, Rubin LJ, Smart FW, Suzuki YJ, Gladwin M, Denholm EM, Gail DB; National Heart, Lung, and Blood Institute Working Group on Cellular and Molecular Mechanisms of Right Heart Failure. Right ventricular function and failure: report of a National Heart, Lung, and Blood Institute working group on cellular and molecular mechanisms of right heart failure. *Circulation*. 2006;114:1883–1891.
3. Vonk Noordegraaf A, Westerhof BE, Westerhof N. The relationship between the right ventricle and its load in pulmonary hypertension. *J Am Coll Cardiol*. 2017;69:236–243.
4. Rudski LG, Lai WW, Afilalo J, Hua L, Handschumacher MD, Chandrasekaran K, Solomon SD, Louie EK, Schiller NB. Guidelines for the echocardiographic assessment of the right heart in adults: a report from the American Society of Echocardiography endorsed by the European Association of Echocardiography, a registered branch of the European Society of Cardiology, and the Canadian Society of Echocardiography. *J Am Soc Echocardiogr*. 2010;23:685–713.
5. Suga H, Sagawa K, Shoukas AA. Load independence of the instantaneous pressure-volume ratio of the canine left ventricle and effects of epinephrine and heart rate on the ratio. *Circ Res*. 1973;32:314–322.
6. Brown KA, Ditchey RV. Human right ventricular end-systolic pressure-volume relation defined by maximal elastance. *Circulation*. 1988;78:81–91.
7. Sunagawa K, Maughan WL, Burkhoff D, Sagawa K. Left ventricular interaction with arterial load studied in isolated canine ventricle. *Am J Physiol*. 1983;245:H773–H780.
8. Brimioulle S, Wauthy P, Ewalenko P, Rondelet B, Vermeulen F, Kerbaul F, Naeije R. Single-beat estimation of right ventricular end-systolic pressure-volume relationship. *Am J Physiol Heart Circ Physiol*. 2003;284:H1625–H1630.
9. Trip P, Kind T, van de Veerdonk MC, Marcus JT, de Man FS, Westerhof N, Vonk-Noordegraaf A. Accurate assessment of load-independent right ventricular

systolic function in patients with pulmonary hypertension. *J Heart Lung Transplant*. 2013;32:50–55.

10. Hsu S, Houston BA, Tampakakis E, Bacher AC, Rhodes PS, Mathai SC, Damico RL, Kolb TM, Hummers LK, Shah AA, McMahan Z, Corona-Villalobos CP, Zimmerman SL, Wigley FM, Hassoun PM, Kass DA, Tedford RJ. Right ventricular functional reserve in pulmonary arterial hypertension. *Circulation*. 2016;133:2413–2422.
11. Brewis MJ, Bellofiore A, Vanderpool RR, Chesler NC, Johnson MK, Naeije R, Peacock AJ. Imaging right ventricular function to predict outcome in pulmonary arterial hypertension. *Int J Cardiol*. 2016;218:206–211.
12. Vanderpool RR, Pinsky MR, Naeije R, Deible C, Kosaraju V, Bunner C, Mathier MA, Lacomis J, Champion HC, Simon MA. RV-pulmonary arterial coupling predicts outcome in patients referred for pulmonary hypertension. *Heart*. 2015;101:37–43.
13. Glower DD, Spratt JA, Snow ND, Kabas JS, Davis JW, Olsen CO, Tyson GS, Sabiston DC, Rankin JS. Linearity of the Frank-Starling relationship in the intact heart: the concept of preload recruitable stroke work. *Circulation*. 1985;71:994–1009.
14. Karunanithi MK, Michniewicz J, Copeland SE, Feneley MP. Right ventricular preload recruitable stroke work, end-systolic pressure-volume, and dP/dtmax-end-diastolic volume relations compared as indexes of right ventricular contractile performance in conscious dogs. *Circ Res*. 1992;70:1169–1179.
15. Inuzuka R, Kass DA, Senzaki H. Novel, single-beat approach for determining both end-systolic pressure-dimension relationship and preload recruitable stroke work. *Open Heart*. 2016;3:e000451.
16. Tedford RJ, Mudd JO, Girgis RE, Mathai SC, Zaiman AL, Housten-Harris T, Boyce D, Kelemen BW, Bacher AC, Shah AA, Hummers LK, Wigley FM, Russell SD, Saggar R, Saggar R, Maughan WL, Hassoun PM, Kass DA. Right ventricular dysfunction in systemic sclerosis-associated pulmonary arterial hypertension. *Circ Heart Fail*. 2013;6:953–963.
17. Senzaki H, Chen CH, Kass DA. Single-beat estimation of end-systolic pressure-volume relation in humans: a new method with the potential for noninvasive application. *Circulation*. 1996;94:2497–2506.
18. Mirsky I, Tajimi T, Peterson KL. The development of the entire end-systolic pressure-volume and ejection fraction-afterload relations: a new concept of systolic myocardial stiffness. *Circulation*. 1987;76:343–356.
19. Regen DM. Calculation of left ventricular wall stress. *Circ Res*. 1990;67:245–252.
20. Milnor WR, Bergel DH, Bargainer JD. Hydraulic power associated with pulmonary blood flow and its relation to heart rate. *Circ Res*. 1966;19:467–480.
21. Team R Development Core Team. *R: A Language and Environment for Statistical Computing*. Vienna, Austria: R Foundation for Statistical Computing; 2008.
22. Karunanithi MK, Feneley MP. Single-beat determination of preload recruitable stroke work relationship: derivation and evaluation in conscious dogs. *J Am Coll Cardiol*. 2000;35:502–513.
23. Sunagawa K, Yamada A, Senda Y, Kikuchi Y, Nakamura M, Shibahara T, Nose Y. Estimation of the hydromotive source pressure from ejecting beats of the left ventricle. *IEEE Trans Biomed Eng*. 1980;27:299–305.
24. Takeuchi M, Igarashi Y, Tomimoto S, Odake M, Hayashi T, Tsukamoto T, Hata K, Takaoka H, Fukuzaki H. Single-beat estimation of the slope of the end-systolic pressure-volume relation in the human left ventricle. *Circulation*. 1991;83:202–212.
25. Lambermont B, Segers P, Ghuysen A, Tchana-Sato V, Morimont P, Dogne JM, Kolh P, Gerard P, D'Orio V. Comparison between single-beat and multiple-beat methods for estimation of right ventricular contractility. *Crit Care Med*. 2004;32:1886–1890.
26. Kass DA, Beyar R, Lankford E, Heard M, Maughan WL, Sagawa K. Influence of contractile state on curvilinearity of in situ end-systolic pressure-volume relations. *Circulation*. 1989;79:167–178.
27. Kelly RP, Ting CT, Yang TM, Liu CP, Maughan WL, Chang MS, Kass DA. Effective arterial elastance as index of arterial vascular load in humans. *Circulation*. 1992;86:513–521.
28. Mahapatra S, Nishimura RA, Sorajja P, Cha S, McGoon MD. Relationship of pulmonary arterial capacitance and mortality in idiopathic pulmonary arterial hypertension. *J Am Coll Cardiol*. 2006;47:799–803.

SUPPLEMENTAL MATERIAL

Data S1. End-systolic pressure volume relationship based on maximum myocardial stiffness

Mirsky et al. demonstrated that the maximal stress–strain ratio (i.e., myocardial stiffness) attained during end-systole is constant throughout acute changes in preload, and that the end-systolic pressure volume relationship (ESPVR) derived from the myocardial stress-strain relationship is curvilinear, representing a more physiologic ESPVR than linear ESPVR.[1] The average fiber stress (σ) can be defined by $\sigma = (3/2) \times P \times V_m / V_{wall}$, where P is the left ventricular pressure, and V_m and V_{wall} are the midwall and wall volumes, respectively. The midwall volume is defined as the logarithmic mean of the chamber volume (V) and the outer volume (V_{out}),$(V_{out} - V) / (\ln V_{out} - \ln V)$.[2] Therefore,

$$V_m = V_{wall} / \ln\left(1 + \frac{V_{wall}}{V}\right). \quad \text{[equation S1]}$$

The midwall natural strain (ε_n) can be defined by $\varepsilon_n = (1/3)\ln(V_m / V_{m0})$, where V_{m0} is the midwall volume at zero stress. We set the systolic zero-stress volume as the reference distension, as described by Mirsky et al.[1] The average fiber strain can be calculated as $\varepsilon = K_m \varepsilon_n$, where K_m is the constant value determined by the assumed geometry of the ventricle.[1] The average systolic myocardial stiffness (E_{av}) is defined as $E_{av} = \sigma / \varepsilon$, and end-systole was defined as the latest time at which the systolic myocardial stiffness reached its maximum value (max E_{av}). The end-systolic, stress–strain relationship (σ_{es} versus ε_{es}) based on the maximal stiffness concept can be represented in the form:

$$\mathrm{MaxE_{av}} = \sigma_{es}/\varepsilon_{es} = (\frac{9}{2K_m}) \times P_{es} \times V_{mes}/(V_{wall} \times \ln(\frac{V_{mes}}{V_{m0}})), \quad \text{[equation S2]}$$

where P_{es} and V_{mes} are the left ventricular pressure and midwall volume at end-systole, respectively.

Rearranging equation S2 results in the following equation:

$$P_{es} = \left(\frac{2K_m}{9}\right) \times \mathrm{maxE_{av}} \times \ln(\frac{V_{mes}}{V_{m0}}) \times V_{wall}/V_{mes} \quad \text{[equation S3]}$$

Converting the midwall volume to the chamber volume using equation S1 yields,

$$P_{es} = \left[\left(\frac{2K_m}{9}\right) \times \mathrm{maxE_{av}}\right] \times \ln(\frac{\ln(1+\frac{V_{wall}}{V_0})}{\ln(1+\frac{V_{wall}}{V_{es}})}) \times \ln(1 + \frac{V_{wall}}{V_{es}}). \quad \text{[equation S4]}$$

Therefore, ESPVR can be expressed in the form:

$$P_{es}(V_{es}) = a \times \ln(\frac{\ln(1+\frac{V_{wall}}{V_0})}{\ln(1+\frac{V_{wall}}{V_{es}})}) \times \ln(1 + \frac{V_{wall}}{V_{es}}), \quad \text{[equation S5]}$$

where a is an amplification factor. Equation S5 can be approximated using the following simpler formula:

$$P_{es}(V_{es}) = A \times \ln(\frac{V_{es}}{V_0}) \times \ln(1 + \frac{V_{wall}}{V_{es}}), \quad \text{[equation S6]}$$

where A is an amplification factor.

Data S2. Relationship between $\acute{E}_a$ and pulmonary impedance

Milnor et al. described that the mean external ventricular work per time (W) can be expressed as a sum of the steady and pulsatile components:[3]

$$W = P_0 Q_0 + \frac{1}{2}\sum_{n=1}^{N} Q_n{}^2 Z_n \cos\ \theta_n, \quad \text{[equation A1]}$$

using the mean values of pressure and volume flow P_0 and Q_0, harmonic components Q_n of the ventricular ejection wave, input impedance Z_n, and phase θ_n. At any given rate, the ratio of each harmonic amplitude to mean flow (Q_n/Q_0) was found to be fairly consistent.[3]

Therefore,

$$Q_n = C_n * Q_0, \quad \text{[equation A2]}$$

where C_n is a function of heart rate. Combined with equation A1,

$$W = P_0 Q_0 + \frac{1}{2} Q_0{}^2 \sum_{n=1}^{N} C_n{}^2 Z_n \cos\ \theta_n, \quad \text{[equation A3]}$$

Stroke work (SW) and stroke volume (SV) can be expressed as

$$SW = W * T_0, \quad \text{[equation A4]}$$

$$SV = Q_0 * T_0, \quad \text{[equation A5]}$$

where T_0 is cycle length. We defined $\acute{E}_a$ as P_m/SV, which is equal to SW/SV^2. Combined with equations A3-A5,

$$\acute{E}_a = SW/SV^2 = \frac{1}{T_0}\left(P_0/Q_0 + \frac{1}{2}\sum_{n=1}^{N} C_n{}^2 Z_n \cos\ \theta_n\right). \quad \text{[equation A6]}$$

Therefore, $\acute{E}_a$ is a global marker of vascular impedance, which inherently accounts for both steady and pulsatile afterloads.

Data S3. R code for our single-beat method

```
#Pres, pressure data of the signal-averaged pressure–volume loop
#Vol, volume data of the signal-averaged pressure–volume loop
#MRIwallv, right ventricular wall volume as measured by cardiac magnetic resonance imaging
#sESV, end-systolic volume of the signal-averaged pressure–volume loop
#sEDV, end-diastolic volume of the signal-averaged pressure–volume loop
#sSW, stroke work of the signal-averaged pressure–volume loop

library(nleqslv)
pp<-min(c(1:length(Pres))[Pres== max(Pres,na.rm=T)][1])
ep<-min(c(1:length(Pres))[Vol== min(Vol, na.rm=T)],na.rm=T)
esp<-NA
pVo<-NA
pa<-NA
pVo[1]<- 0.1*sEDV
pa[1]<-100
for(i in 1:100){Tc<-function(x){log(x/pVo[i])*log(1+(MRIwallv/x))}
maxeav<-max(Pres[pp:ep]/Tc(Vol[pp:ep]),na.rm=T)
esp[i]<-max(c(pp:ep)[Pres[pp:ep]/Tc(Vol[pp:ep])>0.99*maxeav],na.rm=T)
Xs<-Vol[pp: esp[i]]
Ys<-Pres[pp: esp[i]]
fits<-nls(Ys~ a*log(Xs/c)*log(1+(MRIwallv/Xs)),start=c(c=pVo[i],a=pa[i]),trace=T)
pVo[i+1]<-summary(fits)$coefficient[1]
pa[i+1]<-summary(fits)$coefficient[2]}
Vo<-pVo[length(pVo)]
A<-pa[length(pa)]
tPm<-function(x){A*log(x/Vo)*log(1+(MRIwallv/x))}
A2<-sSW/(sEDV-sESV)/(log(sESV/ Vo)*log(1+(MRIwallv/sESV)))
Pm<-function(x){A2*log(x/ Vo)*log(1+(MRIwallv/x))}
Est<-function(Vsw){Msw<-sSW/(sEDV-Vsw)
y<-Pm (Vsw)-Msw}
Vsw<-nleqslv(0.5*sESV,Est)$x
Msw<-sSW/(sEDV-Vsw)
Msw
```

Figure S1. Relationship between conventional and novel indices of right ventricular–pulmonary arterial coupling

Scatterplots comparing multiple-beat E_{es}/E_a ($E_{es}/E_{a(MB)}$) and multiple-beat M_{sw}/P_m ($M_{sw(MB)}/P_m$). The right ventricular–pulmonary arterial coupling ratio in patients with pulmonary hypertension (black points) was significantly lower than that in those without pulmonary hypertension (red points) ($p=0.03$ for $E_{es(MB)}/E_a$ and $p=0.003$ for $M_{sw(MB)}/P_m$). Multiple-beat M_{sw}/P_m had limited values around 0.80–1.0 in those without PH (red points), whereas multiple-beat E_{es}/E_a ranged much more widely.

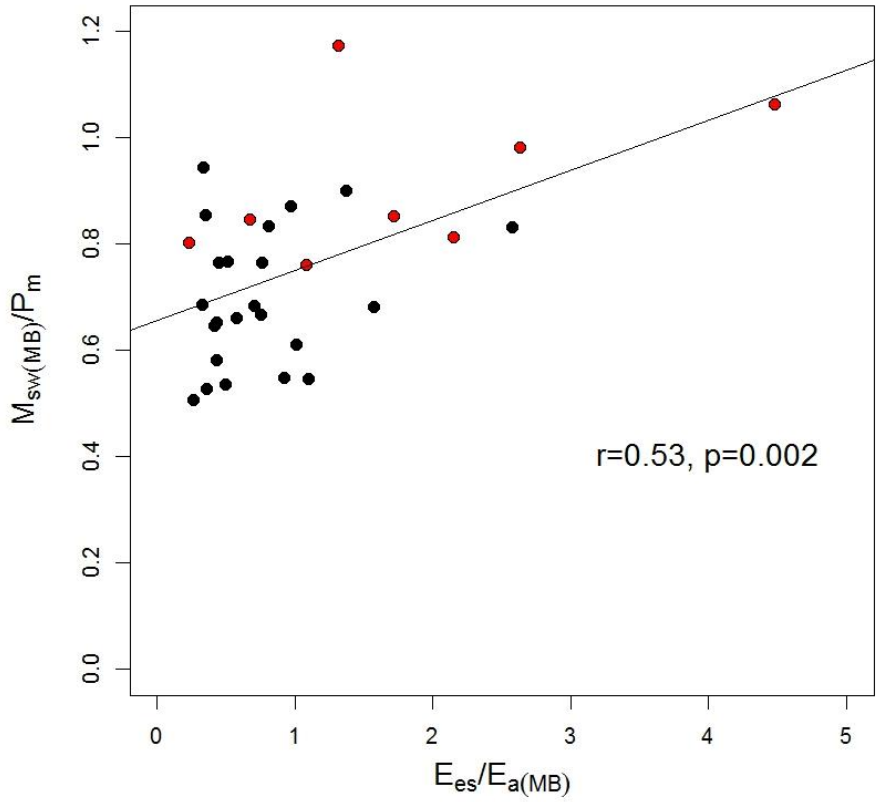

Figure S2. Estimated and measured E'_{es}

A) Scatterplots comparing the estimated and measured E'_{es} (i.e., $M_{sw(SB)}$/stroke volume and $M_{sw(MB)}$/stroke volume) based on measured right ventricular wall volume.

B) Bland–Altman plots for the estimation of E'_{es} based on measured right ventricular wall volume, which shows a mild overestimation by 0.05 (standard error: 0.013) mmHg/mL and limits of agreement from -0.10 to 0.20 mmHg/mL.

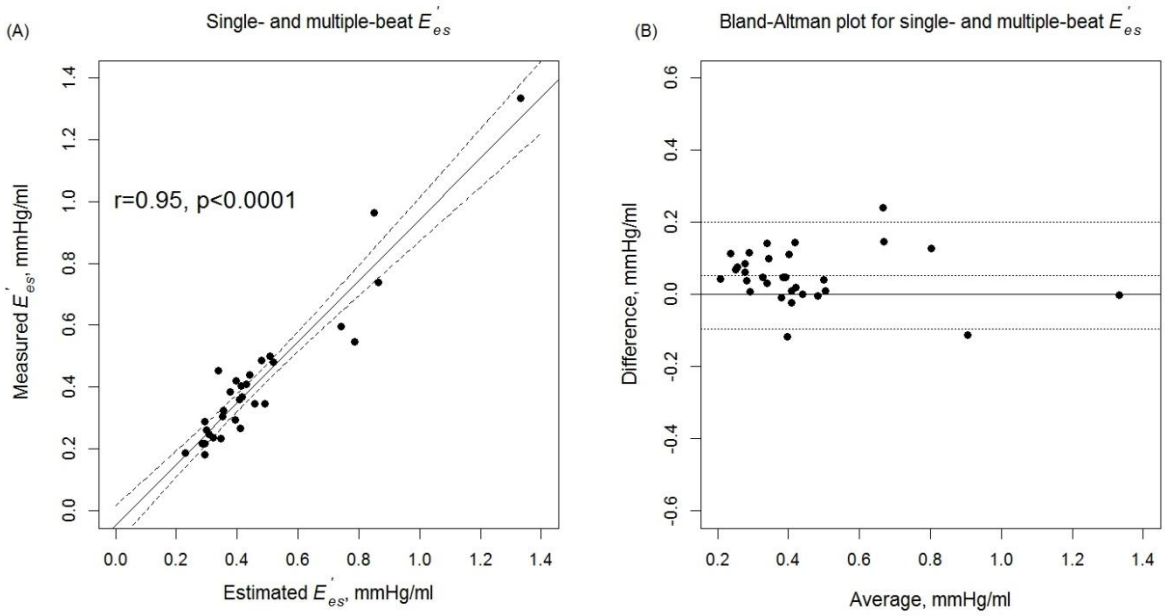

Figure S3. Consistency assessment within multiple-beat data.

Scatterplots comparing the preload recruitable stroke work (PRSW) coefficients estimated as a point on the end-systolic mean ejection pressure–volume relationship (EMPVR) using multiple-beat EMPVR versus the actual multiple-beat PRSW coefficients calculated based on the stroke work-volume plane (i.e., EMPVR-based versus actual $M_{sw(MB)}$ and $V_{sw(MB)}$). These graphs validate the basic principle of the estimation method that point (V_{sw}, M_{sw}) is on the EMPVR curve.

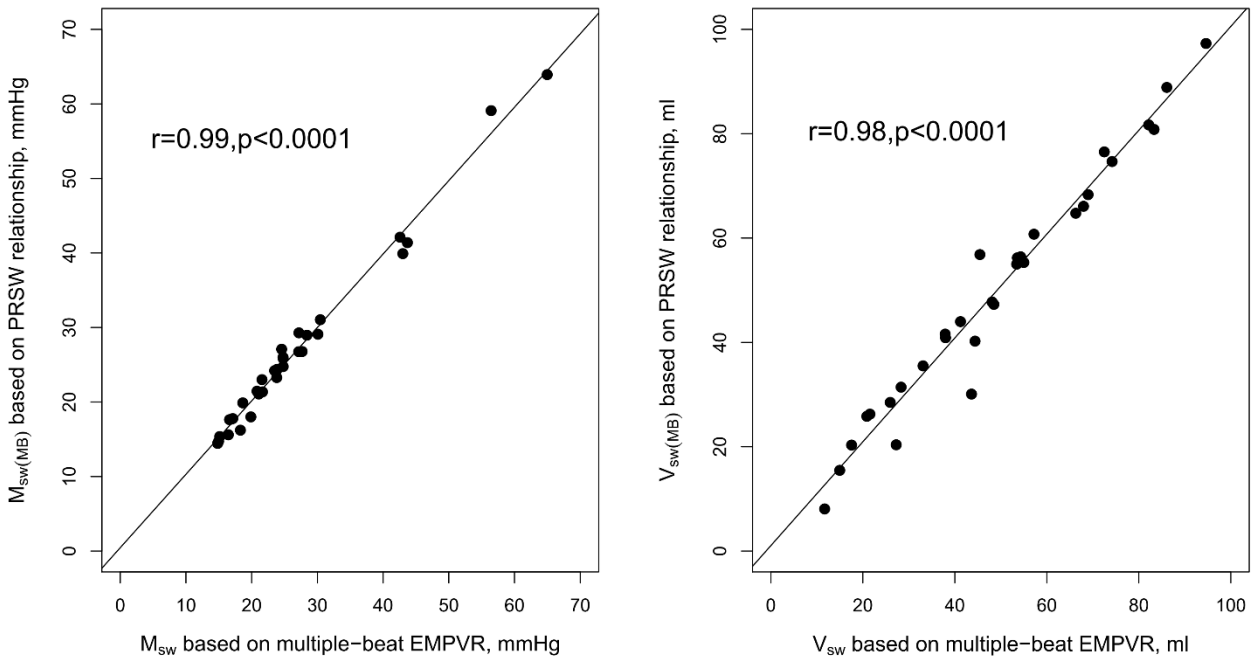

Figure S4. Conventional single-beat estimation of end-systolic elastance (E_{es}) based on sine-wave fit.

Scatterplots comparing single-beat end-systolic elastance (E_{es}) based on the conventional sine-wave method and multiple-beat E_{es} ($E_{es(SB)}$ versus $E_{es(MB)}$).

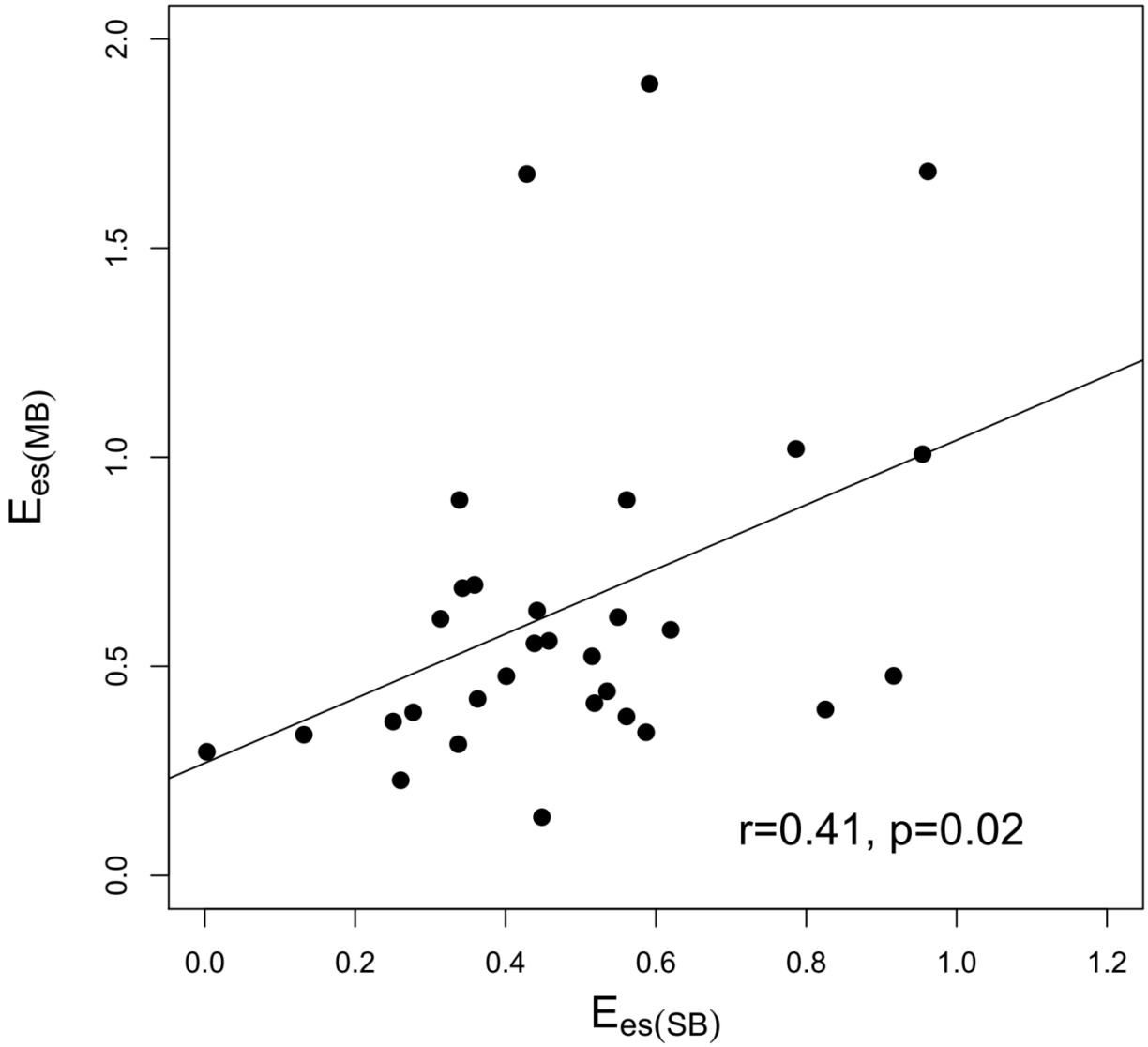

Figure S5. Iterative method used for single-beat estimation of the end-systolic pressure–volume relationship.

(A) The first curve fitting was performed on late systolic points (red open points) based on a randomly selected end-systolic point. The zero-stress volume (V_0, red closed point) was obtained from the estimated end-systolic pressure–volume relationship (ESPVR, red curve), which was used to calculate myocardial stiffness (stress–strain ratio).

(B) Myocardial stiffness was calculated based on the first V_0. The last point attaining the maximal myocardial stiffness (black closed point) was used as the end-systolic point for the second fitting. The second end-systolic point is different from the first randomly selected end-systolic point.

(C) The second curve fitting was performed for the late systolic points determined based on myocardial stiffness (blue open points). The second V_0 (blue closed point) was obtained from the second fitting and was used to calculate myocardial stiffness again. This process was repeated until we identified the end-systolic point that attained the maximal myocardial stiffness, as shown in Figure 1B.

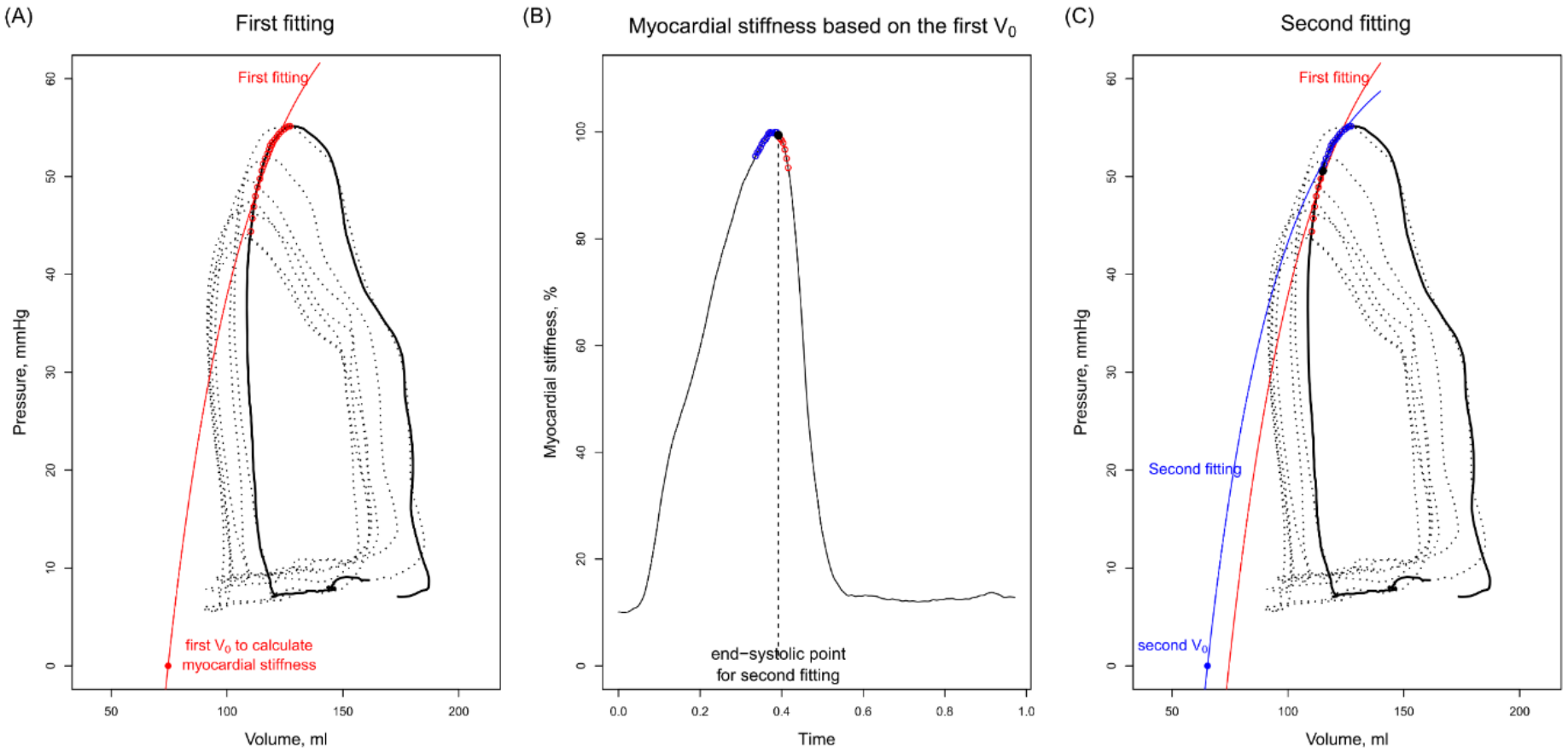
(A)
First fitting
First fitting
first V_0 to calculate
myocardial stiffness
Pressure, mmHg
Volume, ml
(B)
Myocardial stiffness based on the first V_0
Myocardial stiffness, %
end−systolic point
for second fitting
Time
(C)
Second fitting
First fitting
Second fitting
second V_0
Pressure, mmHg
Volume, ml

Supplemental References:

1. Mirsky I, Tajimi T, Peterson KL. The development of the entire end-systolic pressure-volume and ejection fraction-afterload relations: a new concept of systolic myocardial stiffness. *Circulation*. 1987;76:343-56.

2. Regen DM. Calculation of left ventricular wall stress. *Circ Res.* 1990;67:245-52.

3. Milnor WR, Bergel DH, Bargainer JD. Hydraulic power associated with pulmonary blood flow and its relation to heart rate. *Circ Res.* 1966;19:467-80.